Journal of Catalysis **209,** 114–125 (2002)
doi:10.1006/jcat.2002.3605

Oxidation of CO on a Pt/Al_2O_3 Catalyst: From the Surface Elementary Steps to Lighting-Off Tests

II. Kinetic Study of the Oxidation of Adsorbed CO Species Using Mass Spectroscopy

Abdennour Bourane and Daniel Bianchi[1]

Laboratoire d'Application de la Chimie à l'Environnement (LACE), UMR 5634, Université Claude Bernard, Lyon-I, Bat. 303, 43 Bd du 11 Novembre 1918, 69622 Villeurbanne, France

Received November 21, 2001; revised March 9, 2002; accepted March 9, 2002

Experiments in the transient regime using a mass spectrometer as a detector are performed at $T = 300$ K on a 2.9% Pt/Al_2O_3 catalyst to study the oxidation of the linearly adsorbed CO species (denoted L) with several x% O_2/z% Ar/He mixtures (x and z in the range 0.5–4). CO and O_2 adsorption measurements show that the L CO species and a strongly adsorbed oxygen species (denoted O_{sads}) formed by the dissociative chemisorption of O_2 are adsorbed on the same sites of the freshly reduced Pt particles. L CO and O_{sads} species have high heats of adsorption: 115 and 175 kJ/mol, respectively, at full coverage of the Pt surface and do not desorb in helium at a temperature lower than 350 K. Moreover, it is shown that at 300 K a preadsorbed L CO species is not displaced by oxygen adsorption but is converted into CO_2 by a weakly adsorbed oxygen species (denoted O_{wads}) according to the elementary step (denoted S3): $L + O_{wads} \rightarrow CO_2$ (rate constant, k_3). This confirms the conclusion of a previous study performed using FTIR spectroscopy. O and C mass balances during the transient regime reveal (a) that during the first seconds of the transient the oxygen consumption is mainly due to the formation of the O_{wads} species and that its adsorption equilibrium is rapidly attained and (b) that an O_{sads} species is adsorbed for each L CO species removed by oxidation. This leads to a Pt surface where the coverage of the L CO species decreases while that of the O_{sads} species increases with the duration of the oxidation. However, it is shown that the rate of the reaction (denoted S3a), $L + O_{sads}$ species, is significantly lower than that of step S3 and does not contribute to the CO_2 formation in the presence of O_2. A comparison is presented with the literature data on Pt single crystals (UHV studies) and supported Pt catalysts.

1. INTRODUCTION

One of the objectives in gas/solid catalysis is to correlate the rate of a catalytic reaction such as CO/O_2 on supported noble metal catalysts to the elementary steps on the surface of the catalyst. However, for the a priori simple CO/O_2 reaction this correlation is still debated (1–8). For instance, UHV studies on single crystals have shown that the Langmuir–Hinshelwood mechanism between adsorbed CO and an oxygen species (denoted O_{ads}) coming from the dissociative chemisorption of O_2 explains most experimental results at low pressures (7). There is a competitive adsorption of CO and O_2 and the CO/O_2 reaction is detected only for reaction conditions allowing a decrease in the coverage of the adsorbed CO species (7, 9–11). On Pt/Al_2O_3 the adsorption of CO at $T < 373$ K either alone or in the presence of oxygen mainly leads to the formation of a linear CO species (denoted L, IR band at 2070–2080 cm^{-1}) with small amounts of bridged (denoted B) and threefold-coordinated (denoted 3FC) CO species (12, 13). Using FTIR spectroscopy, we have shown (14 and references therein) that at ≈300 K the L CO species is oxidized in CO_2 using x% O_2/He mixtures and that it can be considered an adsorbed intermediate in the CO/O_2 reaction. Moreover, the heat of adsorption of the L CO species linearly varies with its coverage (denoted θ_L), from $E_1 =$ 115 kJ/mol at $\theta_L = 1$ to $E_0 = 206$ kJ/mol at $\theta_L = 0$ (13, 15, 16), indicating that it cannot significantly desorb at $T < 350$ K, as experimentally observed (17, 18). This leads to the conclusion that it is not necessary to consider that the L species must quantitatively desorb to explain its rate of oxidation at $T < 373$ K. The study of the oxidation of the L CO species by FTIR spectroscopy (using several x% O_2/He mixtures) has shown (14) that this reaction proceeds by a surface elementary step that involves a weakly adsorbed oxygen species (denoted O_{wads}) formed without any competition with the L CO species, by the dissociative chemisorption of O_2. It has also been shown (14) that the switch to x% O_2/He → He leads to the immediate interruption of the oxidation of the L species. This means that if a strongly adsorbed oxygen species (denoted O_{sads}) was present on the surface, it did not significantly contribute to the oxidation of the L CO species.

FTIR spectroscopy did not allow us to determine the evolution of the coverage of the O_{wads} and O_{sads} species during

[1] To whom correspondence should be addressed. E-mail: daniel.bianchi@univ-lyon1.fr.

0021-9517/02 $35.00

the oxidation of the L species. In the present study this reaction is studied using experiments in the transient regime with a mass spectrometer as a detector in order (a) to confirm the conclusions of (14), (b) to reveal the presence of O_{wads} and O_{sads} species on the surface during the oxidation of the L CO species, and (c) to compare the rate of oxidation of the L CO species with O_{wads} and O_{sads} species. This analytical procedure has been used by several authors on various Pt-containing solids and Bennett (19) gives a large review of the contribution of this method to the knowledge of several catalytic reactions, in particular CO/O_2. The main originality of the present study is to perform oxygen and carbon mass balances during the experiments in the transient regime to quantify the amounts of oxygen and CO species on the surface of the Pt/Al_2O_3 solid during the reaction and to deduce the coverages of each adsorbed species as well as the rates of the different surface processes.

2. EXPERIMENTAL

The 2.9% Pt/Al_2O_3 catalyst (in weight percent γ-Al_2O_3; BET area, 100 m^2/g; incipient wetness method using $H_2PtCl_6 \cdot xH_2O$) was the same as the one used and characterized in previous studies (13–16). The experiments in the transient regime with a mass spectrometer as a detector have been run with an analytical system previously described (20). Mainly, various valves allowed us to perform switches between regulated gas flows (1 atm total pressure) which passed through the catalyst (powder) contained in a quartz microreactor. A quadrupole mass spectrometer permitted the determination of the composition (molar fraction) of the gas mixture at the outlet of the reactor during a switch, after a calibration procedure using gas mixtures of known compositions. The molar fractions of the gas mixtures in addition to the temperature of the catalyst (K-type thermocouple, $\phi = 0.5$ mm) were determined with an acquisition rate of one analysis each 1.5 s. The gases studied in the present study were H_2, He, CO, O_2, Ar, and CO_2.

Before the adsorption of CO, the 2.9% Pt/Al_2O_3 catalyst was treated *in situ* (100 cm^3/min) at 713 K according to the following procedure: oxygen (30 min) → helium (30 min) → hydrogen (1 h) → helium (10 min) and then cooled in helium to the adsorption temperature. After this treatment, the Pt dispersion on a fresh catalyst was $D = 0.85$ (13–16), in agreement with literature data (21) on similar Pt catalysts. The same catalyst sample was used for several experiments and it was pretreated before each adsorption experiment as described above. However, in (14) before the study of the CO/O_2 reaction by FTIR spectroscopy, the reduced catalyst was initially treated in 1% CO/He from 300 to 713 K for the determination of the heats of adsorption of CO. This led to a decrease in the Pt dispersion to ≈0.6–0.5. Then this dispersion was constant after several cycles of CO adsorption at high temperature/pretreatment (stabilized solid). A similar treatment in 1% CO/He was performed in the present study to stabilize the dispersion.

The oxidation of the L CO species was studied according to the following procedure: after the reduction of the stabilized catalyst, CO was adsorbed at 300 K, performing the switch He → x% CO/z% Ar/He (100 cm^3/min; x and z in the range 0.5–4) during $t_a \approx 2$ min. After a short helium purge (≈60 s) a new switch was performed, He → y% O_2/z% Ar/He (100 cm^3/min; y and z in the range 0.5–4) during a time t_O (oxidation of the adsorbed CO species), while the composition of the gas mixture at the outlet of the reactor was determined with the mass spectrometer. After a duration t_O of the oxidation a new short helium purge was performed followed by a new switch, He → x% CO/z% Ar/He, during a time t_r (reduction of the O_{sads} species). Note that to be sure the data did not concern a particular state of the catalyst, the results were mainly obtained after several cycles of oxidation of the L species/reduction of O_{sads} species (denoted O/R). Racine *et al.* (22) as well as Bennett (19) gave reviews of experiments in the transient regime performed to understand the CO/O_2 reaction in particular on single crystals (10, 23, 24), foil (25), and supported metal catalysts (17, 26–28). However, occasionally the experimental data are used (a) to perform C and O mass balances and (b) to support kinetic models, such as in (29–31).

3. RESULTS AND DISCUSSION

3.1. Adsorption of CO and O_2 on the Pt/Al_2O_3 Catalyst

Figure 1 A gives the evolution of the molar fractions of the gas (excepted He) at the outlet of the reactor during the switch He → 2% CO/2% Ar/He performed at $T_a = 300$ K on the reduced stabilized Pt/Al_2O_3 solid. A temperature peak with a maximum of ≈4 K (not shown) is observed

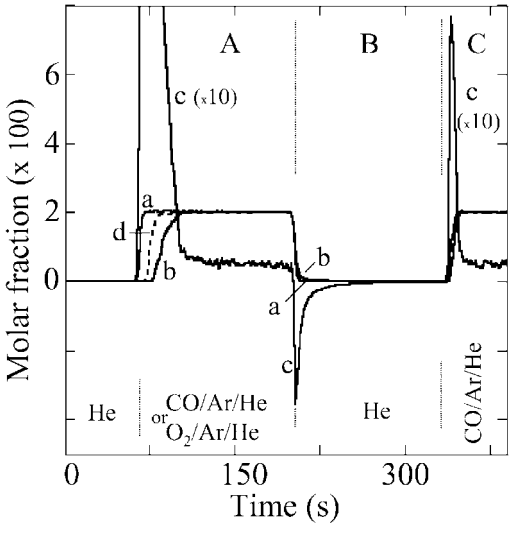

FIG. 1. Adsorption and desorption of CO and O_2 on Pt/Al_2O_3: (a) Ar; (b) CO; (c) (curve a – curve b) × 100; (d) O_2.

during the adsorption, in agreement with the observations of Racine *et al.* (22) on a Pt/Al_2O_3 solid. The total CO uptake, QACO = 78 μmol CO/g ($D \approx 0.54$ with a CO/Pt ratio of 1), is determined from Fig. 1 (for given molar flow rate, F, weight of the catalyst, W, and duration, t_a, of adsorption) by (20):

$$\mathrm{QACO} = \int_0^{t_a} (\text{curve a} - \text{curve b}) \cdot \frac{F}{W} \cdot dt \qquad [1]$$

However, curve c in Fig. 1, which is obtained from (curve a − curve b) × 10 reveals a small CO desorption peak (≈4 μmol/g) in Fig. 1B and then a small readsorption peak (≈4 μmol/g) during a new switch with CO/Ar/He (Fig. 1C), indicating a reversible chemisorption. FTIR spectroscopy studies have shown (13) that the adsorption of CO on the present catalyst leads to a strong IR band at 2070 cm^{-1} ascribed to a L CO species associated with weak IR bands below 2000 cm^{-1} due to B and 3FC CO species. We have determined (13, 15, 16) that the heats of adsorption of the three adsorbed species linearly vary with their coverages: from 206 kJ/mol at $\theta_L = 0$ to 115 kJ/mol at $\theta_L = 1$ for the L species, from 135 kJ/mol at $\theta_{3FC} = 0$ to 115 kJ/mol at $\theta_{3FC} = 1$ for the 3FC species, and from 94 kJ/mol at $\theta_B = 0$ to 45 kJ/mol at $\theta_B = 1$ for the B species. These values indicate that only the B species can significantly desorb at 300 K during the helium purge. The peaks (≈4 μmol of CO/g) in curve c (Figs. 1B and 1C) are probably due to the desorption and readsorption of the B CO species, respectively. The amount of strongly adsorbed CO species is $\mathrm{QACO_{ir}} = 74$ μmol/g.

Curve d in Fig. 1 shows the evolution of the molar fraction of O_2 during the switch to He → 2% O_2/2% Ar/He on the freshly reduced Pt/Al_2O_3 solid (stabilized). A temperature peak of ≈7 K is observed during the O_2 adsorption, indicating that the heat of adsorption of O_2 is higher than that of CO. Curves a and d indicate that 38 μmol/g of O_2 is irreversibly adsorbed (no peaks in Figs. 1B and 1C). Assuming a dissociative chemisorption of O_2 with a ratio O/Pt = 1, the number of Pt sites involved in the adsorption of O_2 is equal to QAO = 76 μmol of O/g of catalyst, in good agreement with QACO = 78 μmol/g, as observed on Pt/SiO_2 (17) and on single crystals (32, 33). This leads to the conclusion that on the present Pt/Al_2O_3 catalyst CO and O_2 are adsorbed on the same Pt sites. The irreversible amount of adsorbed CO is mainly due to the formation of the L CO species with a low contribution of 3FC species (14) while the irreversible amount of adsorbed oxygen is ascribed to a strongly adsorbed O species (denoted O_{sads}). This justifies that in the present study we identify the amount of irreversibly adsorbed CO ($\mathrm{QACO_{ir}} = 74$ μmol/g) to the L CO species, which is strongly adsorbed (13). The activation energy of desorption of the O_{sads} species at high coverage has been determined using a TPD procedure. After the adsorption of O_2 at 300 K (Fig. 1d) the temperature of the catalyst T_d is increased in a helium flow from 300 to ≈980 K (50 K/min). Figure 2A shows that O_2 does not appear in the gas flow before 820 K. At $T_d = 976$ K, the total amount of O_2 desorbed is 4.8 μmol of O_2/g (decrease in the coverage from 1 to 0.87). To determine the heat of adsorption of the O_{sads} species at full coverage of the Pt surface, we use the mathematical formalism of the ITPD (intermittent temperature-programmed desorption) procedure (34–36). The rate of desorption of O_{sads} is given by

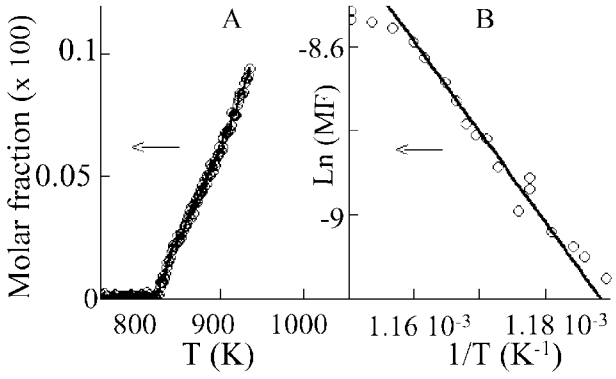

FIG. 2. Determination of the activation energy of desorption of O_2 on the reduced Pt/Al_2O_3 catalyst using ITPD procedure. (A) Molar fraction (MF) of O_2 during the TPD; (B) $\ln(\mathrm{MF}) = f(1/T)$.

$$v_d = \frac{-d\theta}{dt} = k_d \cdot \theta^2 = \upsilon \cdot \theta^2 \cdot \exp\left(-\frac{E_d(\theta)}{R \cdot T}\right), \qquad [2]$$

where k_d is the rate constant of desorption, ν is the frequency factor, and $E_d(\theta)$ is the activation energy of desorption depending on the coverage. In an ITPD procedure (34–36) it is considered that if θ is roughly constant (i.e., at the beginning of the desorption process when $\theta \approx 1$ and readsorption is not significant) then expression [2] leads to

$$\left.\frac{d\ln(v_d)}{d\left(\frac{1}{T}\right)}\right|_\theta = \frac{-E_d(\theta)}{R}. \qquad [3]$$

The rate of desorption, v_d, is proportional to the molar fraction (denoted MF) of O_2 (Fig. 2A) and the slope of $\ln(\mathrm{MF}) = f(1/T)$ (Fig. 2B) for θ varying from 1 to 0.97 (beginning of the desorption peak) indicates an activation energy of desorption of 175 ± 10 kJ/mol at $\theta_{Osads} \approx 1$, in agreement with 199 ± 27 kJ/mol, determined by Wartnaby *et al.* (37) on Pt (110) at high coverage of the surface. Olsson *et al.* (38) find a lower value (142 kJ/mol) by classical TPD on 7.7% Pt/Al_2O_3 (38). The above results show that for high coverages of the Pt surface, the heat of adsorption of the L species (115 kJ/mol) is lower than that of the O_{sads} species (175 kJ/mol) considering that the adsorption of O_2 is not activated. However, with CO/O_2 gas mixtures the Pt surface is mainly covered by the L CO species (39 and references therein).

3.2. *Composition of the Gas Mixtures during Oxidation of the L CO Species*

After the adsorption of CO according to the experiments in Fig. 1, a switch to He → 2% O_2/4% Ar/He permits the oxidation the L CO species for a duration t_O. Figure 3A gives the evolutions of the molar fractions of the gases at the outlet of the reactor during the switch. The rate of the CO_2 production is given by

$$RCO_2 = (\text{curve c}) \times \frac{F}{W}. \qquad [4]$$

The total amount of CO_2 formed during the isothermal oxidation ($QCO_{2iO} = 40\ \mu$mol/g) at 300 K is obtained by

$$QCO_{2iO} = \int_0^{t_O} RCO_2 \cdot dt. \qquad [5]$$

QCO_{2iO} is lower than $QACO_{ir} = 74\ \mu$mol/g because the rate of the CO_2 production decreases with time on stream (in particular with the decrease in the coverage of the L species (14, 40)) and cannot be followed with accuracy for large values of t_O. However, the increase in the temperature of the catalyst from 300 to 420 K in 2% O_2/4% Ar/He (temperature-programmed oxidation (TPO) ≈50 K/min) leads to a peak of CO_2 production (Fig. 3B) with a maximum at 345 K. The total amount of CO_2 produced, 74 μmol/g, during the isothermal oxidation (40 μmol/g) and the TPO (34 μmol/g) is in good agreement with $QACO_{ir}$. This indicates that there is no significant amount of CO species remaining on the surface after the TPO. The total amount of O_2 consumed during the TPO (Fig. 3B, curve b) is 34 μmol of O_2/g compared to the CO_2 production (34 μmol/g); this indicates that a strongly adsorbed oxygen species is formed for each L CO species removed by oxidation. Note the absence of a temperature peak during the isothermal oxidation of the L CO species (curve d, Fig. 3A).

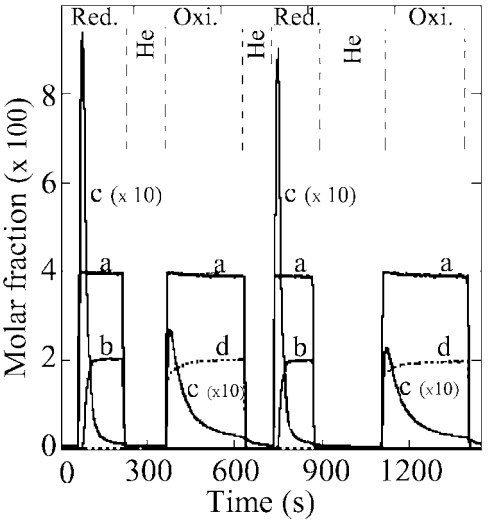

FIG. 4. Consecutive reduction/oxidation cycles of the adsorbed species using 2% CO/4% Ar/He and 2% O_2/4% Ar/He: (a) Ar; (b) CO; (c) CO_2; (d) O_2.

Figure 4 gives the molar fractions of the gases during two consecutive reduction/oxidation cycles (denoted R/O) at 300 K using 2% CO/4% Ar/He and 2% O_2/4% Ar/He mixtures after at least three previous R/O cycles. Figure 5 gives similar results for 0.5% CO/0.5% Ar/He and 0.5% O_2/1% Ar/He. Figures 4 and 5 prove the good reproducibility of the data during several consecutive cycles and they indicate that the rate of the CO_2 production is higher during

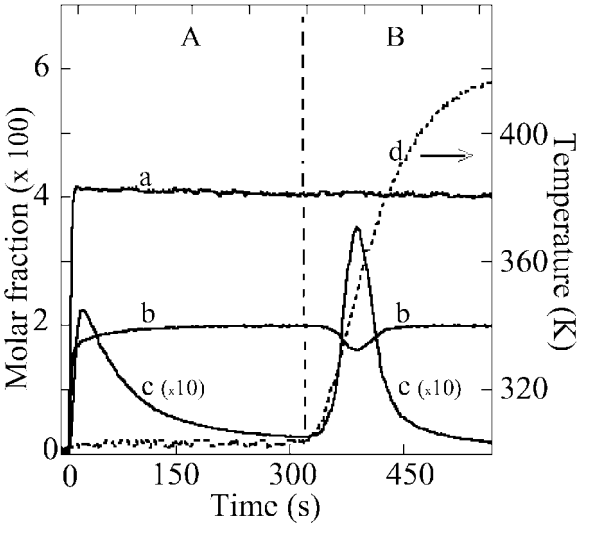

FIG. 3. Isothermal (A) and temperature-programmed (B) oxidation of the L CO species: (a) Ar; (b) O_2; (c) CO_2; (d) temperature of the catalyst.

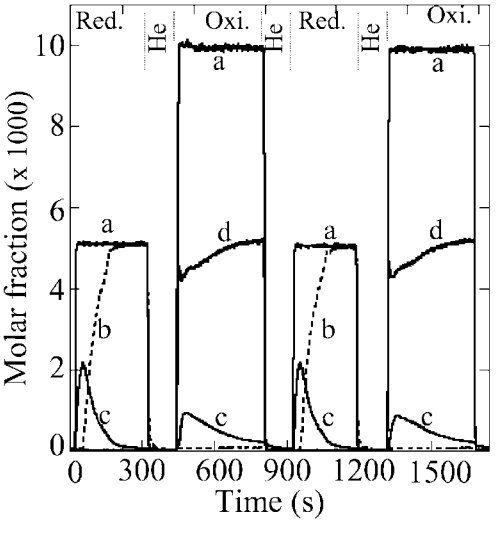

FIG. 5. Consecutive reduction/oxidation cycles of the adsorbed species using 0.5% CO/0.5% Ar/He and 0.5% O_2/1% Ar/He: (a) Ar; (b) CO; (c) CO_2; (d) O_2.

the reduction steps than during the oxidation steps for the same P_{CO} and P_{O2} values. This is discussed in a forthcoming paper (41) while the present study is focused on the oxidation step. The exploitation of the data in Figs. 3–5 is based on C and O mass balances. Note that (a) there is no significant CO desorption during the oxidation processes in Figs. 3–5, indicating the absence of competition between L CO and adsorbed oxygen species—L CO species only is removed from the surface by oxidation—and (b) the CO_2 production depends on the P_{O2} partial pressure (compare Figs. 4 and 5). During the isothermal oxidation several parameters can be determined as a function of the duration t of the reaction. The evolution of the coverage of the L CO species θ_L is given by

$$\theta_L(t) = 1 - \frac{\int_0^t R\mathrm{CO}_2 \cdot dt}{\mathrm{QACO}_{ir}} \quad \text{where } 0 \le t \le t_O. \qquad [6]$$

The evolution of the rate of the total O_2 consumption (oxidation of the L CO species and oxygen adsorption) is given by

$$R\mathrm{O}_2\mathrm{C} = (\alpha \cdot \text{curve a} - \text{curve b}) \cdot \frac{F}{W}, \qquad [7]$$

where $\alpha = 2/4$ for the experiment in Fig. 3 (the total amount of O_2 consumed, QO_2C, is obtained by integrating RO_2C between 0 and t_O). The evolution of the net rate of the oxygen adsorption (weakly and strongly adsorbed oxygen species) is given by

$$R\mathrm{O}_{ads} = 2 \times R\mathrm{O}_2\mathrm{C} - R\mathrm{CO}_2. \qquad [8]$$

The total amount of oxygen adsorbed during the oxidation (QAO_O in micromoles of O per gram) is obtained by integrating RO_{ads} between 0 and t_O.

3.3. On the Confirmation of the Conclusions of Ref. (14)

The adsorption of CO on Pt/Al_2O_3 mainly leads to the L CO species (13, 14) and this justifies the fact that the CO_2 production in the present study is attributed to its oxidation. Using expression [6], $\theta_L(t)$ can be determined for various O_2 partial pressures changing the x value in the $x\%$ $O_2/z\%$ Ar/He mixtures (i.e., Figs. 4 and 5). Figure 6 shows $\theta_L(t)$ for $x = 0.5$, 1, 2 and it confirms the impact of P_{O_2} on the rate of oxidation (14). It has been shown (14) that in a large range of θ_L values $\ln(\theta_L) = f(t)$ is a straight line for various P_{O_2} values because the L CO species is oxidized by an elementary step (denoted step S3) involving a weakly adsorbed oxygen species, O_{wads}, formed without competition with the L CO species:

$$\text{(S3)} \quad \mathrm{L} + \mathrm{O}_{wads} \rightarrow \mathrm{CO}_{2ads} \quad \text{with a rate constant } k_3.$$

The rate of desorption of CO_2 is considered as fast (7). The evolution of the coverage θ_L of the L species during its

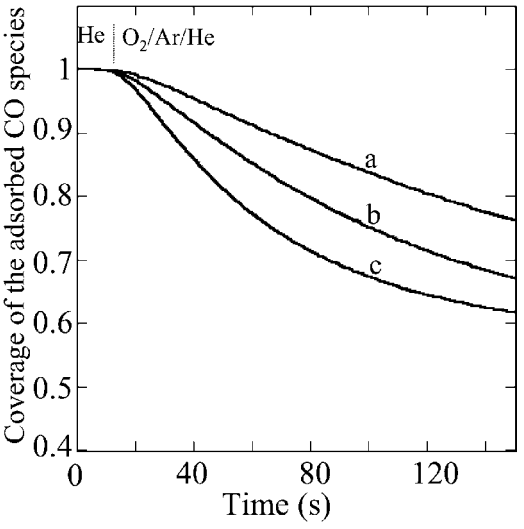

FIG. 6. Evolution of the coverage of the L species which several partial pressures of O_2: (a) 500 Pa; (b) 1000 Pa; (c) 2000 Pa.

oxidation is given by

$$\frac{-d\theta_L}{dt} = k_3 \cdot \theta_L \cdot \theta_{Owads}, \qquad [9]$$

where θ_{Owads} is the coverage of the O_{wads} species. Assuming that θ_{Owads} is constant during oxidation then expression [9] shows that $\ln(\theta_L) = f(t)$ is a straight line, as observed in (14). From curves in Fig. 6, similar straight lines are observed (not shown) and their slopes provide the apparent rate constants $k_{ap} = k_3\theta_{Owads}$ at 300 K, i.e., 0.58×10^{-2} s^{-1} and 0.22×10^{-2} s^{-1} for $P_{O_2} = 2000$ and 500 Pa, respectively, in reasonable agreement with (14). Using several P_{O_2} values in the range of $(500 - 10^5)$ Pa, it has been observed (14) that $k_{ap} = f(P_{O_2}^{0.5})$ is a straight line. This has been explained by the fact that the oxygen species involved in the oxidation of the L species is weakly adsorbed and that its coverage according to Langmuir's model can be approximate to

$$\theta_{wads} = \frac{\left(K_{O_2} \cdot P_{O_2}\right)^{0.5}}{1 + \left(K_{O_2} \cdot P_{O_2}\right)^{0.5}} \approx \left(K_{O_2} \cdot P_{O_2}\right)^{0.5}, \qquad [10]$$

where K_{O_2} is the adsorption coefficient for the O_{wads} species ($K_{ap} = k_3 K_{O_2}^{0.5} P_{O_2}^{0.5}$). With the results of the present study a similar straight line has been observed leading to $k'_{ap} = k_3 K_{O_2}^{0.5} = 1.2 \times 10^{-4}$ s^{-1} Pa$^{-0.5}$, in good agreement with that determined using FTIR spectroscopy, 2.8×10^{-4} s^{-1} Pa$^{-0.5}$ (14). Finally the present study confirms our previous conclusions (14): the L CO species is oxidized in the presence of O_2 by a surface elementary step involving a weakly adsorbed oxygen species, O_{wads}, formed by the dissociation of O_2 without competition with the L CO species. Note that it has been shown (14, 40) that the apparent rate constant decreases with the decrease in θ_L for $\theta_L < \approx 0.3$, probably due to an increase in the activation energy of step S3 with the decrease in θ_L (40). This participates in the decrease

in the rate of the CO_2 production during the oxidation at 300 K and explains the necessity of performing a TPO to oxidize the totality the L CO species (Fig. 3B).

3.4. *On the Presence of O_{wads} and O_{sads} Species during the Isothermal Oxidation*

In (14) the presence of O_{wads} species was only deduced from the kinetic study while that of the O_{sads} species was speculative. From the present results the presence of two oxygen species on the Pt surface can be experimentally proved. Figure 7 shows the evolutions of the rates of (a) total O_2 consumption (RO_2C, expression [7]; Fig. 7a), (b) adsorption of oxygen (RO_{ads}, expression [8]; Fig. 7b), and (c) CO_2 production (RCO_2, expression [4], Fig. 7c) during an isothermal oxidation with 2% O_2/4% Ar/He. It can be observed that in the first seconds of the transient the main part of the oxygen consumption is due to the adsorption of oxygen (curves a and b are overlapped), indicating that oxygen is adsorbed without significant removal of the L CO species. This supports the conclusion on the absence of competition between O_{wads} and L CO species. Note that the small delay between the Ar signal and the appearance of CO_2 during the oxidation is not due to a significant irreversible adsorption of CO_2 on the alumina support because it is observed whatever the number of O/R cycles (see below the comments on the adsorption of CO_2). Moreover, as the CO_2 production does not increase in parallel with the O_2 signal this indicates that a Eley–Rideal mechanism is improbable for the oxidation of the L CO species, as considered by other arguments in (14).

During the final part of the oxidation (Fig. 7) there is an equality between RO_{ads} (curve b) and RCO_{2O} (curve c) because an O_{sads} species is formed for each L CO species removed (similarly to what was observed during the TPO shown in Fig. 3). Starting from a Pt surface mainly covered by the L CO species, the oxidation reaction progressively leads to a surface covered by the L CO and O_{sads} species. The results in Fig. 7 clearly show that there are two types of adsorbed oxygen species on the surface during the oxidation: (a) a weakly adsorbed oxygen species, O_{wads}, formed without any competition with the L CO species and involved in the oxidation of the L CO species, and (b) a strongly adsorbed oxygen species, O_{sads}, formed on the sites liberated by the oxidation of the L species. Note that the O_{wads} species seems associated with the presence of adsorbed CO species on the Pt surface because in Fig. 1B we did not detect significant reversible adsorbed oxygen species during the O_2 chemisorption on reduced Pt particles. The net rate of adsorption of the O_{wads} species, RO_{wads}, with the duration of oxidation can be evaluated (curve d in Fig. 7) considering that an O_{sads} species is formed for each L CO species oxidized: $RO_{wads} = RO_{ads} - RCO_{2iO}$. It can be observed that RO_{wads} (Fig. 7d) presents a sharp peak during the first seconds of the oxidation, indicating the rapid attainment of the adsorption equilibrium (around during the time needed to observe a constant molar fraction of Ar). The integration with time on stream of curve d in Fig. 7 indicates an amount of O_{wads} species $QO_{wads} \approx 11$ μmol/g for $P_{O_2} = 2000$ Pa. Compared to the total number of Pt sites this represents a small coverage of the Pt surface, in agreement with the fact that this species is weakly adsorbed. At the present time we do not know the location of the sites adsorbing the O_{wads} species. However, it must be remembered that the B CO species rapidly desorbs at 300 K (Fig. 1B), creating some empty Pt sites where maybe oxygen is weakly adsorbed. The amount of O_{wads} species with $P_{O_2} = 500$ Pa (Fig. 5) is $QO_{wads} \approx 5$ μmol/g, clearly indicating that QO_{wads} increases with P_{O_2}, as expected for a weakly adsorbed O_2 species.

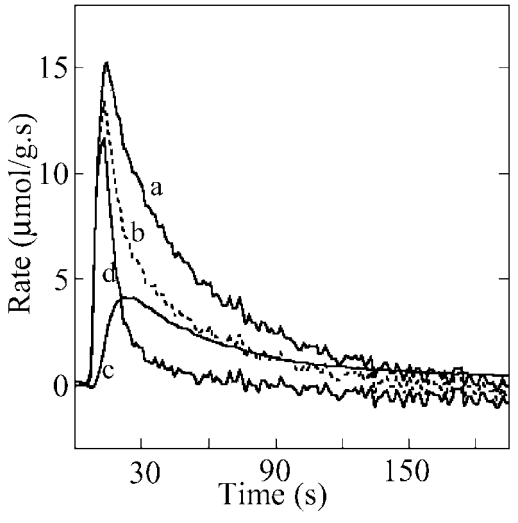

FIG. 7. Evolution of the rates of several processes during the isothermal oxidation of the L CO species at 300 K: (a) rate of oxygen consumption; (b) net rate of oxygen adsorption; (c) rate of CO_2 formation; (d) net rate of adsorption of the O_{wads} species.

The above C and O mass balances have been performed after several O/R cycles to prevent the influence of the CO_2 chemisorption on the Al_2O_3 support. The impact of this CO_2 adsorption has been evaluated studying the adsorption of 0.6% CO_2/1% Ar/He on the reduced Pt/Al_2O_3 solid (experiments, not shown, similar to those in Fig. 1). The total amount of adsorbed CO_2 is 25 μmol/g with 6 μmol/g of reversible chemisorption. The irreversible adsorption of CO_2 (19 μmol/g) indicates that during the first oxidation of the L CO species a fraction of the CO_2 production can be irreversibly adsorbed on the support (various carbonates). This explains that C and O mass balances have been performed after several O/R cycles to saturate the sites of the support. The observation of a reversible CO_2 chemisorption (6 μmol/g with $P_{CO_2} = 600$ Pa) indicates that there is an uncertainty about the C and O mass balances during the oxidation of the L CO species, leading to the QO_{wads} values, because this CO_2 adsorption has been

neglected. However, the CO_2 partial pressure during the oxidation with $P_{O_2} = 2000$ Pa is small, $P_{CO_2} \approx 20$ Pa at the maximum of the rate of the CO_2 production (see Figs. 3 and 4), and the amount of reversibly adsorbed CO_2 species must be significantly lower than 6 μmol/g determined with $P_{CO_2} = 600$ Pa. Indeed, during a helium treatment after the oxidation of ≈50% of the L CO species a small production (≈2 μmol/g) of CO_2 is detected (see Fig. 4). However, this is probably due to several processes, such as the desorption of the weakly adsorbed CO_2 species on alumina, the CO_2 formation from steps S3 (with the residual O_2 during the first seconds of the transient), and maybe the reaction between L CO species and O_{sads} species (see below). This means that the QO_{wads} value must be considered to be in the range ≈9–11 μmol/g for $P_{O_2} = 2000$ Pa.

3.5. *On the Reaction between L CO and O_{sads} Species*

By using FTIR spectroscopy we have observed that the oxidation of the L species is immediately stopped after a switch to 2% O_2/He → He (see Fig. 7 in (14)). We concluded that if there were some O_{sads} species on the surface they were not significantly active for the oxidation of the L CO species. The curves b and d in Fig. 7 clearly prove that O_{sads} species are formed during the progressive removal of the L CO species, leading to a situation where L CO and O_{sads} species are present on the Pt surface. The following experiment performed after several O/R cycles confirms that the reaction L + O_{sads} → CO_2 (denoted step S3a) does not significantly contribute to the removal of the L CO species at 300 K in the presence of O_2. After a switch to He → 2% O_2/4% Ar/He during a short period (Fig. 8A) a purge in helium is performed. Figure 8B shows that there

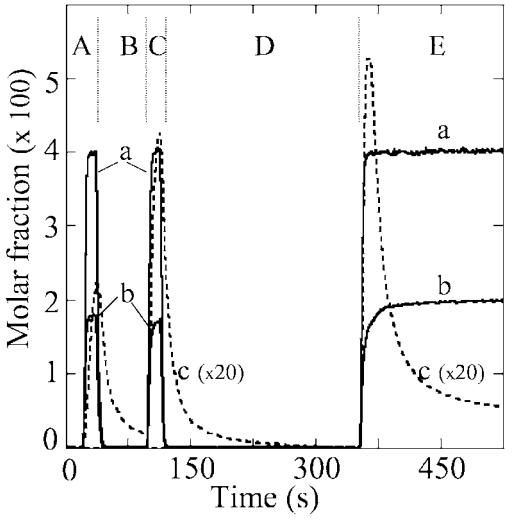

FIG. 8. Interrupted oxidation of the L CO species at 300 K using switches between He and 2% O_2/4% Ar/He: (a) Ar; (b) O_2; (c) CO_2. (A) He → 2% O_2/4% Ar/He; (B, D) in helium; (C, E) in 2% O_2/4% Ar/He.

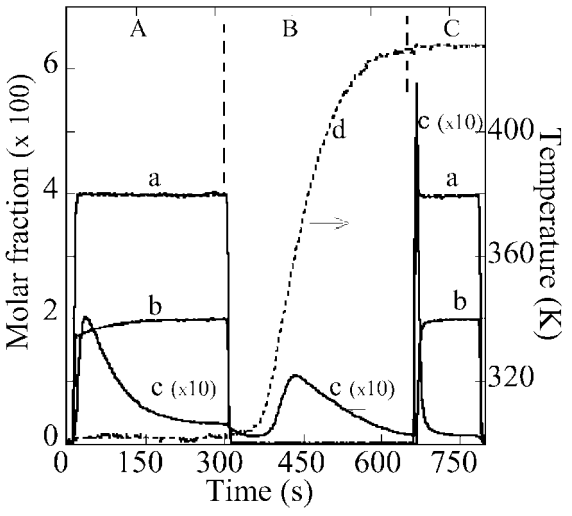

FIG. 9. Oxidation of the L CO species at several temperatures: (a) Ar; (b) O_2; (c) CO_2; (d) temperature of the catalysts. (A) Isothermal oxidation at 300 K with 2% O_2/4% Ar/He; (B) TPSO in helium; (C) isothermal oxidation at 428 K with 2% O_2/4% Ar/He.

is a strong decrease in the CO_2 production during the He purge (in part due to the CO_2 desorption from the Al_2O_3 support) while the reintroduction of O_2 (Fig. 8C) leads to a high rate of CO_2 production. A purge in helium for 4 min (Fig. 4D) has no impact on the CO_2 production during oxidation with O_2 (Fig. 8E). These observations are in agreement with similar experiments by FTIR spectroscopy (14). The above results confirm that the rate of oxidation of the L CO species at 300 K in the absence of gaseous O_2 is not significant compared to that observed in the presence of O_2. Moreover, the C and O mass balances during the reintroduction of O_2 also reveal the formation of O_{wads} species (as observed in Fig. 7), indicating that this species desorbs during the helium purge. The O_{sads} species formed on the sites liberated by the oxidation of the L CO species are not significantly active for the CO_2 production compared to the O_{wads} species. However, the experiments in Fig. 9 show that CO_2 can be produced by step S3a at $T > 300$ K. After the oxidation at 300 K of the L CO species with a 2% O_2/4% Ar/He mixture (Fig. 9A) to decrease the coverage of the L CO species to $\theta_L \approx 0.53$ and to increase that of the O_{sads} species to $\theta_{Osads} \approx 0.47$, the solid is heated (≈50 K/min) in helium from 300 to 493 K (temperature-programmed surface oxidation (TPSO)). It can be observed in Fig. 9B that a CO_2 peak is detected with a maximum at 361 K, proving that step S3a occurs during the TPSO. The amount of CO_2 produced during the TPSO experiment, 25 μmol/g, indicates that some L CO species remain on the Pt surface. However, introducing 2% O_2/4% Ar/He at 428 K (Fig. 9C) leads to a high rate of CO_2 production (7.5 μmol/g), indicating the removal of the remaining adsorbed L CO species. These results show that step S3a, involving the O_{sads} species,

does not proceed with a high rate compared to that of step S3, involving the O_{wads} species formed in the presence of O_2. Note that a strongly adsorbed species means that at $T \approx 300$ K, it does not desorb in an inert gas at the opposite of a weakly adsorbed species which depends on the partial pressure. However, there are a priori no correlations between weakly and strongly adsorbed species and active or inactive species.

A fraction of the CO_2 formed during the increase in the temperature in He (Fig. 9B) may come from the desorption of carbonate species on the Al_2O_3 support, formed by the CO_2 production during the previous O/R cycles. To evaluate the contribution of this process, after the adsorption of CO_2 at 300 K using a 0.6% CO_2/1% Ar/He mixture a TPD experiment (300–480 K) is performed (not shown), leading to a small CO_2 peak (5 μmol/g from the 19 μmol/g irreversibly adsorbed at 300 K) with a maximum at 346 K. This indicates that in Fig. 9 the CO_2 production during the TPSO is mainly produced by step S3a. The above results (Figs. 8 and 9) show that at 300 K the reaction between L CO and O_{sads} proceeds at a low rate and does not significantly contribute to the CO_2 production in the presence of O_2 (which is only due to step S3).

Finally the present results confirm our previous conclusions (14) on the mechanism of the oxidation of the L CO species: mainly, this species is oxidized at 300 K according to step S3. In addition, it is demonstrated that (a) in the first seconds of the experiment the O_2 consumption is due to the formation of the O_{wads} species (the adsorption equilibrium is rapidly established); (b) an O_{sads} species is formed during the removal of the L CO species by its oxidation; and (c) this O_{sads} species is not significantly active for the oxidation of the L CO species compared to the O_{wads} species. In a forthcoming study (41) we apply the same analytical procedure to study the reduction by CO gas of the strongly adsorbed O_{sads} species (reduction steps in Figs. 4 and 5).

3.6. Comparison of the Present Results with UHV Studies

Similarly to UHV studies (7) our study has shown that the L CO species is oxidized by O_2 following a Langmuir–Hinshelwood mechanism. The Eley–Rideal mechanism is not operative, in agreement, for instance, with the isotopic study of Matsushima (25). The main difference with the UHV views of the CO/O_2 reaction is that we consider that the oxidation of the L CO species involves a weakly adsorbed oxygen species formed without competition with the L CO species while UHV studies (7) show that CO must desorb to create some free sites for the adsorption of oxygen. The desorption of the L CO species seems improbable at room temperature on Pt/Al_2O_3 because its heat of adsorption at high coverage is too high to permit a significant desorption in the short period of its oxidation at 300 K, as performed in the present study, in agreement with previous studies (17, 18). Moreover, Fig. 3 clearly shows that O_2 does not displace the L CO species (no CO production) even if the heat of adsorption of O_2 is significantly higher than that of CO on the freshly reduced Pt particles. This absence of competition is in agreement with the UHV studies that consider that CO must desorb to permit the adsorption of O_2 (7). There are maybe no contradictions between the present study and the UHV conclusions considering the two experimental conditions (pressure gap).

Figure 9 shows, in agreement with UHV studies, that there is a reaction between the L CO species and an O_{sads} species (step S3a) formed on the sites liberated by the oxidation of the L CO species by O_{wads} species (and not by desorption, as considered in UHV studies). However, the rate of step S3a is significantly lower than that of steps S3 and does not significantly contribute to the CO_2 production at 300 K in the presence of O_2 (a ratio of >10 between two rates of reaction is enough to neglect the lower rate). The reverse is probably true in UHV studies, which use very low oxygen partial pressures. The apparent rate of step S3 depends on $P_{O_2}^{0.5}$: $k_{ap} = k_3\ \theta_0 = k'_{ap}\ P_{O_2}^{0.5} = 2.8 \times 10^{-4}\ P_{O_2}^{0.5}$ (14) at 300 K. Low P_{O_2} values may lead to a situation where the rate of step S3a becomes higher than that of step S3. For instance, in UHV conditions, the O_2 partial pressures are $\approx 10^{-4}$ Pa (7, 25, 42), leading to $k_{ap} = 2.8 \times 10^{-6}\ s^{-1}$, while we use $P_{O_2} > 2000$ Pa, giving $k_{ap} = 1.3 \times 10^{-2}\ s^{-1}$. The expected k_{ap} values in UHV conditions may change the ratio between the rates of steps S3 and S3a, leading to a situation where step S3a dominates the CO_2 production.

Moreover, on the present Pt/Al_2O_3 catalyst the L CO species cannot desorb to liberate some sites for O_2 chemisorption (due to a high heat of adsorption). However, the heat of adsorption of the B CO species is low (45 kJ/mol at $\theta_B = 1$) and this adsorbed species rapidly desorbs at 300 K during a short helium purge (Fig. 1). The Pt sites liberated by the removal of the B CO species probably are those involved in the formation of O_{wads} species without any competition with L CO species. The diversity of the sites, which may exist on a supported Pt catalyst, is maybe a second cause of the difference with the UHV studies (material gap). However, it must be noted that on Pt(100) it has been observed that oxidation of preadsorbed CO by O_2 can be realized even at high CO coverages (42) and the authors conclude (see comments on Fig. 24 in (42)) that "most probably because a small number of defect sites are not so effectively blocked by adsorbed CO and allow oxygen adsorption." This last comment is in agreement with our conclusion that some Pt sites (i.e., those adsorbing the B CO species) are free for the oxygen adsorption without competition with the L CO species. Moreover, the fact that L and O_{wads} species are adsorbed on different Pt sites is in agreement with the IRAS observations of Xu and Yates (43) on Pt(335). The authors conclude that the most reactive geometry in the CO/O_2 reaction involves oxygen adsorbed

on step sites with CO adsorbed on terrace sites, supporting the view that two types of Pt sites are involved in the CO/O_2 reaction, as considered in the present study.

The presence of the most active oxygen species, O_{wads}, for the oxidation of the L CO species depends on the oxygen partial pressure and in that sense is strongly different than the O_{sads} species formed either on the clean Pt surface or after removing the L CO species by oxidation. This seems in agreement with the conclusions of Wartnaby *et al.* (37) on Pt(110). The authors have studied the heats of reaction during either CO reacting with preadsorbed oxygen (O_{ads} titration) or O_2 reacting with preadsorbed CO (CO_{ads} titration) by using a single-crystal adsorption microcalorimeter. By comparing the measured heat deposited in the crystal with that expected for the reaction, the excess energy removed by the desorbing CO_2 molecules was deduced. The authors have observed, in agreement with previous studies (37 and references therein), that the CO_2 molecules remove more energy (52 kJ/mol) than expected for thermally accommodated molecules during the CO_{ads} titration and only 9 kJ/mol during O_{ads} the titration. The authors suggest that the much greater degree of excitation of CO_2 for the CO_{ads} titration could be due to the channeling of energy from dissociation of oxygen molecules to the product CO_2 via "hot" oxygen adatoms which never thermally accommodate to the surface (37). However, the removal of the CO_{ads} during the titration produces fresh adsorption sites for the adsorption of strongly adsorbed oxygen species (37), as observed in the present study. Yoshinobu and Kawai (44) consider, in agreement with other studies (see references in (44)), that before being accommodated to the surface these nascent (or hot) oxygen atoms are the reactive species on the CO oxidation on Pt(111) at $T < 400$ K while ordered oxygen atoms are unreactive.

3.7. Comparison of the Present Results with Similar Studies on Supported Noble Metal Catalysts

The results in Figs. 3–5 on the oxidation of preadsorbed CO species by O_2 showing the almost immediate production of CO_2 agree well with some studies performed on supported noble metal catalysts (45–47). However, they differ from other studies (17, 26, 27), which observe a large induction period (i.e., 109 s at 353 K on 1% Pt/SiO_2 (26)), before the appearance of CO_2 or the disappearance of the L CO species. This induction period is mainly interpreted with the UHV views, considering that a fraction of the adsorbed CO species must desorb to allow the adsorption of O_2. However, Dwyer and Bennett (17) on 9.1% Pt/SiO_2 have shown that this induction period strongly depends on the experimental conditions. For instance, at 393 K the increase in the flow rate of a 2% O_2/Ar mixture from 9.5 to 114 cm^3/min decreases the induction time from ≈35 to 5 s. This is interpreted (17) by the dependence of the net desorption rate of adsorbed CO on the residual CO partial pressure in the reactor. This means that during the induction period the desorption of the CO species allowing the adsorption of O_2 is considered in a pseudoadsorption equilibrium (18 and references therein). This is only valid if it is assumed that the desorbing species has a not very high heat of adsorption. This agrees with the views of the present study because B and L CO species have strongly different heats of adsorption and only the coverage of the B CO species can be significantly affected by the residual CO partial pressure.

Zhou and Gulari (26) have shown on Pd/Al_2O_3 that increasing the duration of the He purge before the introduction of the O_2-containing mixture strongly decreases the induction period but without any effect on the amount of CO_2 produced during the titration. They suggest that this is due to a restructuring of the adsorbed CO or to reconstruction of the catalyst surface without any desorption. However, this is maybe due to the desorption of an adsorbed CO species present in a small amount on the surface (maybe below the accuracy of the analytical procedure in (26)) with a heat of adsorption significantly lower than the main adsorbed CO species which is strongly adsorbed. These comments associated with the fact that the most active oxygen species is adsorbed without competition show that the induction period observed during the isothermal oxidation of preadsorbed CO on supported noble metal catalysts seems linked to the desorption of an adsorbed CO species with a heat of adsorption significantly lower than that of the adsorbed species which is oxidized during the experiment (the L CO species on Pt-containing catalysts). This allows us to believe that the differences in the profiles of the CO_2 production during the isothermal oxidation at low temperatures of the L CO species on Pt-containing catalysts is maybe due to small differences in the minor adsorbed CO species, such as the B CO species. For instance, if the heat of adsorption of this species is higher on some Pt solids its rate of desorption significantly decreases, leading to an increase in the time needed to liberate the site for the oxygen adsorption. This situation may lead to the observation of an induction period during the oxidation. Simple calculations based on a rate constant of desorption of an adsorbed CO species, $k_d = 10^{13} \exp(-E_d/RT)$, show that for $E_d < 70$ kJ/mol the Pt sites are rapidly liberated (<2 s) by desorption at 300 K while this time strongly increases for $E_d > 80$ kJ/mol. We may expect that if the amount of B CO species on a Pt-containing solid is very low or if its heat of adsorption is >80 kJ/mol at high coverage then the rate of oxidation of the L CO species may present an induction period.

3.8. Kinetic Model and Mobility of the Adsorbed Species

It has been shown that the LH mechanism is involved in the oxidation of the L CO species according to step S3 and Eq. [9]. Expression [9] implicitly assumes that the two

adsorbed species are significantly intermixed on the surface. For instance, it is known that CO can be adsorbed in large amount on Pt(111) precovered by oxygen species (48) and references therein. Szabo *et al.* (49) have suggested that CO can be adsorbed on on-top sites at the middle of the triangle formed by oxygen atoms. On a surface precovered by a L CO species, there is maybe a similar situation and the significant amount of O_{wads} species is perhaps associated with Pt sites close to those adsorbing the L CO species. However, expression [9] also corresponds to the mean-field treatment of the CO/O_2 reaction (50) that justifies the uniform distribution, considering that the diffusion of the adsorbed species is rapid compared to the surface reaction (50, 51). The comparison between the two rates (diffusion versus reaction) mainly depends on their activation energies because the preexponential factor for surface diffusion is close to that of the LH step (51). The rate of diffusion of CO on Pt surfaces (single crystals, foils, and clusters) is considered fast (51, 52), with corrugation ratios $\Omega = E(\text{diffusion})/E(\text{desorption})$ in the range 0.2–0.4 (52). For instance, activation energy of diffusion of CO on Pt(111) is in the range 16–30 kJ/mol (51, and references therein). This value is significantly lower than the activation energy of the LH surface reaction in the range 60–80 kJ/mol (14, and references therein). For the diffusion of the oxygen species the situation is debated (51) because the activation energies of diffusion on Pt surfaces are in the range 41–125 kJ/mol while density functional theory calculations predict 54 kJ/mol (51, 52, and references therein). However, we have shown that the presence of L CO species on the Pt surface strongly changes the oxygen adsorption properties. This is maybe also true for the mobility of the O_{wads} species involved in step S3a that can be higher than that of the oxygen species formed on a clean Pt surface. Ziff *et al.* (53), on a lattice-gas model for the CO/O_2 reaction using Monte Carlo simulations, consider a rapid surface reaction as compared to the diffusion (ZGB model). At the difference of the present study, they indicate that there is an induction period for the CO_2 production during the transient behavior of the surface from a high coverage by CO (low activity) to a high coverage by O (high activity). This indicates that mobile adsorbed species are probably involved on the present catalyst, supporting the mean-field approximations. Note that the diffusion of an adsorbed species such as CO is not incompatible with a model of localized species for the adsorption (54, 15).

At 300 K, it has been shown that some adsorbed O species (O_{sads}) may remain on the surface in the presence of L CO species (they react at higher temperatures). To differentiate these species from the very reactive O_{wads} species, two elementary steps, S3 and S3a, have been considered. Zaera *et al.* (48), studying on Pt(111) the reaction between preadsorbed oxygen with CO, also observe two oxygen species with different reactivity. In particular, at 300 K, an "unreactive" O species can be present on the surface in the presence of L CO species similarly to the O_{sads} species. We have observed similar results on the present Pt/Al_2O_3 catalyst for the O_{sads} reduction by CO (41) (O_{sads} formed by adsorption of O_2). At 300 K, after either L CO oxidation with O_2 or O_{sads} reduction with CO (Figs. 4 and 5) there is a surface state with the presence of both L CO and O_{sads} species. The authors (48) interpret the presence of the "unreactive" O species by considering that the more clustered the oxygen atoms are at the beginning of the kinetic runs, the more likely more oxygen atoms will be removed before reaching the point where only isolated species remain on the surface (unreactive species). They translate this view of the process by considering that the activation energy of the LH step at the surface significantly changes with the coverages of the two adsorbed L CO and O_{ads} species. We have also considered (14) that there is a slight increase in the activation energy of step S3 with the decrease in the coverage of the L CO species for $\theta_L < 0.3$ ($E_3 + 10\,\theta_L$). Finally, the difference in the interpretation of "unreactive" O species on Pt surfaces between the present study and that of Zaera *et al.* (48) is that the authors adopt the view that there is a continuous increase in the activation energy of a LH step involving the same adsorbed species while we consider that the significant difference in the activation energies justifies the separation in elementary steps S3 and S3a. In the present study other properties differentiate the two O species: O_{wads} is formed without competition with the L CO species and its amount depends on P_{O_2} while O_{sads} is formed by the removal of the L CO species and it does not desorb in a inert gas at 300 K. The O_{sads} species is maybe related to the subsurface oxygen, O_s, formed during the CO_{ads} titration by O_2 on Pt surfaces (55). This O_s species is more strongly bound than O_{ads} species (55). This is maybe also true for the activation energies of their reduction by CO.

4. CONCLUSIONS

The following conclusions are derived from the present study on a 2.9% Pt/Al_2O_3 catalyst.

(a) CO and O_2 are strongly adsorbed on the same Pt sites of the reduced solid. Adsorption of CO mainly gives a L CO species.

(b) At high coverage of the surface, O_2 is more strongly adsorbed (O_{sads} species, $E_d = 175$ kJ/mol) than the L CO species ($E_d = 115$ kJ/mol). However, O_2 does not displace preadsorbed L CO species.

(c) The L CO species is oxidized in CO_2 at a temperature lower than 350 K in the presence of x% O_2/y% Ar/He mixture with x in the range 0.5–4.

(d) The oxidation of the L species follows the Langmuir–Hinshelwood mechanism with a weakly adsorbed O_{wads} species formed by the dissociative chemisorption of oxygen without competition with the L CO species. The Eley–Rideal mechanism does not operate. The elementary

step (denoted S3) which controls the oxidation of the L species is $L + O_{wads} \rightarrow CO_{2\ ads}$

(e) Oxygen and carbon mass balances during the oxidation of the L CO species clearly prove the formation of O_{wads} species during the first seconds of the transient experiments and indicate that an O_{sads} species is formed for each L CO species removed by oxidation.

(f) L CO species can be oxidized into CO_2 by the O_{sads} species according to step S3a, $L + O_{sads} \rightarrow CO_2$, but with a rate of reaction significantly lower than that of step S3.

5. NOMENCLATURE

5.1. Amounts of Adsorbed Species

QACO: total amount of adsorbed CO species at 300 K on a freshly reduced solid

$QACO_{ir}$: total amount of irreversibly adsorbed CO species at 300 K

QAO: total amount of strongly adsorbed O species on a freshly reduced solid

QCO_{2iO}: CO_2 formed during the isothermal oxidation of the L CO species

QO_2C: total amount of O_2 consumed during the isothermal oxidation

QAO_O: total amount of oxygen adsorbed during the isothermal oxidation

QO_{wads}: amount of weakly adsorbed oxygen species

5.2. Rates of Processes Involved in the Oxidation of the L CO Species

RCO_{2O}: rate of the CO_2 production during the isothermal oxidation

RO_2C: rate of total O_2 consumption

RO_{ads}: net rate of oxygen adsorption (weakly and strongly adsorbed O species)

RO_{wads}: net rate of adsorption of the weakly adsorbed O species

ACKNOWLEDGMENTS

We acknowledge with pleasure the FAURECIA Industries, Bois sur prés, 25 550 Bavans, France, for its financial support and the M.E.R.T. (Ministère de l'Education Nationale de la Recherche et de la Technologie) for the research fellowship of A. Bourane.

REFERENCES

1. Nibbelke, R. H., Campman, M. A. J., Hoebink, J. H. B. J., and Marin, G. B., *J. Catal.* **171**, 358 (1997).
2. Wojciechowski, B. W., and Aspey, S. P., *Appl. Catal. A.* **190**, 1 (2000).
3. Herz, R. H., and Marin, S. P., *J. Catal.* **65**, 281 (1980).
4. Harold, M. P., and Garske, M. E., *J. Catal.* **127**, 524 (1991).
5. Cai, Y., Strenger, H. G., Jr., and Lyman, C. E., *J. Catal.* **161**, 123 (1996).
6. Thormählen, P., Skoglundh, M., Fridell, E., and Anderson, B., *J. Catal.* **188**, 300 (1999).
7. Engel, T., and Ertl, G., *Adv. Catal.* **28**, 1 (1979).
8. Razon, L. F., and Schmitz, R. A., *Catal. Rev.–Sci. Eng.* **28**, 89 (1986).
9. Shigeishi, R. A., and King, D. A., *Surf. Sci.* **75**, L 397 (1978).
10. Bowker, M., Jones, I. Z., Bennett, R. A., and Poulston, S., *Stud. Surf. Sci. Catal.* **116**, 431 (1998).
11. Szanyi, J., and Goodman, D. W., *J. Phys. Chem.* **98**, 2972 (1994).
12. Barth, R., Pitchai, R., Anderson, R. L., and Verykios, X. E., *J. Catal.* **116**, 61 (1989).
13. Bourane, A., Dulaurent, O., and Bianchi, D., *J. Catal.* **196**, 115 (2000).
14. Bourane, A., and Bianchi, D., *J. Catal.* **202**, 34 (2001).
15. Chafik, T., Dulaurent, O., Gass, J. L., and Bianchi, D., *J. Catal.* **179**, 503 (1998).
16. Dulaurent, O., and Bianchi, D., *Appl. Catal. A* **196**, 271 (2000).
17. Dwyer, S. M., and Bennett, C. O., *J. Catal.* **75**, 275 (1982).
18. Bourane, A., Dulaurent, O., Chandes, K., and Bianchi, D., *Appl. Catal.* **214**, 193 (2001).
19. Bennett, C. O., *Adv. Catal.* **44**, 329 (2000).
20. Bourane, A., Dulaurent, O., and Bianchi, D., *J. Catal.* **195**, 406 (2000).
21. Sharma, S. B., Miller, J. T., and Dumesic, J. A., *J. Catal.* **148**, 198 (1994).
22. Racine, B. N., Sally, M. J., Wade, B., and Herz, R. K., *J. Catal.* **127**, 307 (1991).
23. Conrad, H., Ertl, G., and Küppers, J., *Surf. Sci.* **76**, 323 (1978).
24. Pasteur, A. T., Guo, X. C., Ali, T., Gruyters, M., and King, D. A., *Surf. Sci.* **366**, 564 (1996).
25. Matsushima, T., *J. Catal.* **55**, 337 (1978).
26. Zhou, X., and Gulari, E., *Langmuir* **2**, 709 (1986).
27. Li, Y. E., Boecker, D., and Gonzalez, R. D., *J. Catal.* **110**, 319 (1988).
28. Su, E. C., Rothschild, W. G., and Yao, H. C., *J. Catal.* **118**, 111 (1989).
29. Gass, J. L., and Bianchi, D., *J. Catal.* **123**, 298 (1990).
30. Ahlafi, H., Bennett, C. O., and Bianchi, D., *J. Catal.* **133**, 83 (1992).
31. Nawdali, M., Ahlafi, H., Pajonk, G. M., and Bianchi, D., *J. Mol. Catal.* **162**, 274 (2000).
32. Bonzel, H. P., and Ku, R. J., *Surf. Sci.* **33**, 91 (1972).
33. Ducros, R., and Merrill, R. P., *Surf. Sci.* **55**, 227 (1976).
34. Joly, J. P., *C. R. Acad. Sci. Paris* **295-II**, 717 (1982)
35. Habenschaden, E., and Küppers, J., *Surf. Sci.* **138**, L 147 (1984).
36. Joly, J. P., Méhier, C., Béré, K. E., and Abon, M., *Appl. Catal.* **169**, 55 (1998).
37. Wartnaby, C. E., Stuck, A., Yeo, Y. Y., and King, D. A., *J. Chem. Phys.* **102**, 1855 (1995).
38. Olsson, L., Westerberg, B., Persson, H., Fridell, E., Skoglundh, M., and Anderson, B., *J. Phys. Chem. B* **103**, 10433 (1999).
39. Bourane, A., Dulaurent, O., and Bianchi, D., *Langmuir* **17**, 5496 (2001).
40. Cant, N. W., and Donaldson, R. A., *J. Catal.* **71**, 320 (1981).
41. Bourane, A., and Bianchi, D., in preparation.
42. Imbihl, R., Cox, M. P., and Ertl, G., *J. Chem. Phys.* **84**, 3519 (1984).
43. Xu, J., and Yates, J. T., Jr., *J. Chem. Phys.* **99**, 725 (1993).
44. Yoshinobu, J., and Kawai, M., *J. Chem. Phys.* **103**, 3220 (1995).
45. Sarkany, J., Bartok, M., and Gonzalez, R. D., *J. Catal.* **81**, 347 (1983).

46. Nibbelke, R. H., Nievergeld, A. J. L., Hoebink, J. H. B. J., and Marin, G. B., *Appl. Catal. B* **19**, 245 (1998).
47. Pavlova, S. N., Sadykov, V. A., Razdobarov, V. A., and Paukshtis, E. A., *J. Catal*. **161**, 507 (1996).
48. Zaera, F., Liu, J., and Xu, M., *J. Chem. Phys*. **106**, 4204 (1997).
49. Szabo, A., Kiskinova, M., and Yates, J. J. T., *J. Chem. Phys*. **90**, 4604 (1989).
50. Imbihl, R., and Ertl, G., *Chem. Rev*. **95**, 697 (1995).
51. Zhdanov, V. P., and Kasemo, B., *Surf. Sci. Rep*. **39**, 25 (2000).
52. Seebauer, E. G., and Allen, C. E., *Prog. Surf. Sci*. **49**, 265 (1995).
53. Ziff, R. M., Gulari, E., and Barshad, Y., *Phys. Rev. Lett*. **56**, 2553 (1986).
54. Tompkins, F. C., "Chemisorption of Gases on Metal." Academic Press, London, 1970.
55. von Oertzen, A., Mikhailov, A., Rotermund, H. H., and Ertl, G., *Surf. Sci*. **350**, 259 (1996).